

# Dalton Transactions

Accepted Manuscript



This is an *Accepted Manuscript*, which has been through the Royal Society of Chemistry peer review process and has been accepted for publication.

*Accepted Manuscripts* are published online shortly after acceptance, before technical editing, formatting and proof reading. Using this free service, authors can make their results available to the community, in citable form, before we publish the edited article. We will replace this *Accepted Manuscript* with the edited and formatted *Advance Article* as soon as it is available.

You can find more information about *Accepted Manuscripts* in the [Information for Authors](#).

Please note that technical editing may introduce minor changes to the text and/or graphics, which may alter content. The journal's standard [Terms & Conditions](#) and the [Ethical guidelines](#) still apply. In no event shall the Royal Society of Chemistry be held responsible for any errors or omissions in this *Accepted Manuscript* or any consequences arising from the use of any information it contains.

## Substituent directed selectivity in anion recognition by a new class of simple osmium-pyrazole derived receptor

Ankita Das, Prasenjit Mondal, Moumita Dasgupta, Nand Kishore\* and Goutam Kumar Lahiri\*

*Department of Chemistry, Indian Institute of Technology Bombay, Powai, Mumbai-400076, India. E-mail: [lahiri@chem.iitb.ac.in](mailto:lahiri@chem.iitb.ac.in)*

†Electronic supplementary information (ESI) available: X-ray crystallographic file for [1]ClO<sub>4</sub> and [2]ClO<sub>4</sub> in CIF format, mass spectra (Figs. S1, S9), Mulliken spin density (Fig. S2), colorimetry (Fig. S3), pK<sub>a</sub> plot (Fig. S4), UV-vis plots (Fig. S5), NMR (Figs. S6-S8), log K plots (Fig. S10), DFT optimised structures (Figs. S11-S12), bond parameters (Tables S1-S2) and DFT data (Tables S3-S13). CCDC nos. 1430164 ([1]ClO<sub>4</sub>), 1430165 ([2]ClO<sub>4</sub>).

## Abstract

The present article deals with the structurally, spectroscopically and electrochemically characterised osmium-bipyridyl derived complexes  $[(bpy)_2Os^{II}(HL_1)Cl]ClO_4$  [**1**]ClO<sub>4</sub> and  $[(bpy)_2Os^{II}(HL_2)Cl]ClO_4$  [**2**]ClO<sub>4</sub> incorporating neutral and monodentate pyrazole derivatives (HL) with one free NH function (bpy = 2,2'-bipyridine, HL<sub>1</sub> = pyrazole, HL<sub>2</sub> = 3,5-dimethylpyrazole). The crystal structures of [**1**]ClO<sub>4</sub> and [**2**]ClO<sub>4</sub> reveal intramolecular hydrogen bonding interaction between the free NH proton of HL and the equatorially placed Cl<sup>-</sup> ligand (N-H...Cl) with donor-acceptor distances of 3.114(7) Å and 3.153(6) Å as well as intermolecular hydrogen bonding interaction between the NH proton and one of the oxygen atoms of ClO<sub>4</sub><sup>-</sup> (N-H...O) with donor-acceptor distances of 2.870(10) Å and 3.024(8) Å, respectively. The effect of hydrogen bonding interactions has translated into the less acidic nature of the NH proton of the coordinated HL with estimated  $pK_a > 12$ . **1**<sup>+</sup> and **2**<sup>+</sup> exhibit reversible Os(II)/(III) and irreversible Os(III)/(IV) processes in CH<sub>3</sub>CN within  $\pm 2.0$  V *versus* SCE. The effect of 3,5-dimethyl substituted HL<sub>2</sub> in **2**<sup>+</sup> has been reflected in the appreciable lowering (40 mV) of Os<sup>II/III</sup> potential, along with further decrease in acidity of the NH proton ( $pK_a > 13.0$ ) with regard to HL<sub>1</sub> coordinated **1**<sup>+</sup> ( $pK_a$ : ~12.3). The electronic spectral features of Os(II) (**1**<sup>+</sup>/**2**<sup>+</sup>) and electrochemically generated Os(III) (**1**<sup>2+</sup>/**2**<sup>2+</sup>) derived complexes have been analysed by TD-DFT calculations. The efficacy of **1**<sup>+</sup> and **2**<sup>+</sup> encompassing free NH proton towards the anion recognition process has been evaluated by different experimental investigations using a wide variety of anions. It however establishes that receptor **1**<sup>+</sup> can recognise both F<sup>-</sup> and OAc<sup>-</sup> in acetonitrile solution, while **2**<sup>+</sup> is exclusively selective for the F<sup>-</sup> ion.

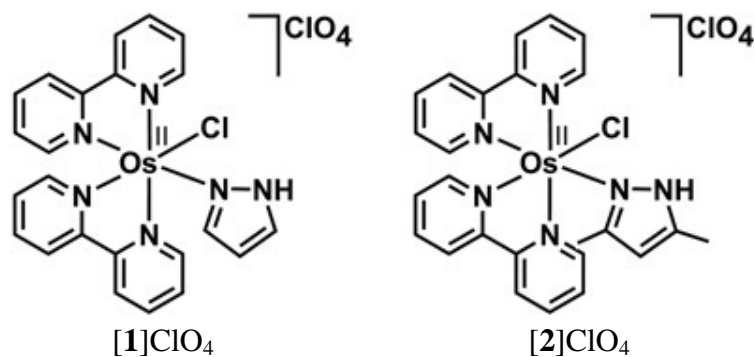
## Introduction

Selective recognition of anion(s) by suitably designed receptor is an important chemical event since anions play vital roles in various chemical, biological and environmental processes.<sup>1</sup> A wide variety of receptors for the anion recognition process in aprotic solvents, involving hydrogen bonding interaction and Bronsted acid-base chemistry is well documented in literature.<sup>2</sup> One of the commonly adopted approaches towards the fabrication of effective receptor for the anion sensing process includes the development of metal complex framework encompassing one or more ligands embedded with free NH function(s).<sup>3</sup> The complex mode of non-covalent interactions between the receptor and anion could however be efficiently monitored by different experimental techniques in combination with theoretical insights.<sup>4</sup> The strong metal-ligand charge transfer transition in the lower energy visible region as well as facile electron-transfer process within the accessible solvent potential window make the transition metal derived receptors rather attractive<sup>5</sup> as compared to otherwise popular organic based receptors such as urea, thiourea, imidazole ion, amide, phenol.<sup>2d,3c,5</sup>

In this regard, ruthenium-polypyridyl (2,2'-bipyridine (bpy), 1,10-phenanthroline (phen), 2,2':6',2'-terpyridine (trpy)) derived frameworks incorporating active ligands with free NH proton(s) have been established as effective receptors for selective anions.<sup>6</sup> The examples of analogous osmium based complexes as possible receptor for selected anion(s) are however limited to a few recent reports.<sup>6f-g,7</sup>

This indeed is the genesis of the present article demonstrating structural and spectroelectrochemical aspects of two newly designed osmium-bipyridine derived complexes  $[(bpy)_2Os^{II}(HL_1)Cl]ClO_4$  [1]ClO<sub>4</sub> and  $[(bpy)_2Os^{II}(HL_2)Cl]ClO_4$  [2]ClO<sub>4</sub> (Scheme 1) involving pyrazole derivatives, HL<sub>1</sub> = pyrazole, HL<sub>2</sub> = 3,5-dimethylpyrazole with one free NH proton of

varying acidity. The present exploration with a series of anions such as  $F^-$ ,  $Cl^-$ ,  $Br^-$ ,  $I^-$ ,  $OAc^-$ ,  $SCN^-$ ,  $NO_3^-$ ,  $HSO_4^-$ ,  $H_2PO_4^-$  via the combination of different experimental techniques and DFT calculations has revealed a unique feature of  $2^+$  in contrast to  $1^+$  towards the selective recognition of  $F^-$  ion.



**Scheme 1** Representation of complexes.

Though pyrazole derived osmium systems are available in literature,<sup>8</sup> to the best of our knowledge the present article demonstrates for the first time the use of the osmium-pyrazoles,  $1^+$  and  $2^+$  towards the recognition of anions with special reference to the remarkable impact of substituent (H ( $1^+$ ) versus Me ( $2^+$ )) on the exclusive selectivity process.<sup>9</sup>

## Results and discussion

### Synthesis, general characterisation and crystal structures

The mononuclear complexes  $[(\text{bpy})_2\text{Os}^{\text{II}}(\text{HL}_1)\text{Cl}]\text{ClO}_4$ , **[1]** $\text{ClO}_4$  and  $[(\text{bpy})_2\text{Os}^{\text{II}}(\text{HL}_2)\text{Cl}]\text{ClO}_4$ , **[2]** $\text{ClO}_4$  (bpy = 2,2'-bipyridine,  $\text{HL}_1$  = pyrazole,  $\text{HL}_2$  = 3,5-dimethylpyrazole) have been synthesised in fairly good yield from the precursor complex *cis*- $[\text{Os}^{\text{II}}(\text{bpy})_2(\text{Cl})_2]$  and  $\text{HL}_1$  or  $\text{HL}_2$ , in refluxing 1:1 ethanol-water under dinitrogen atmosphere followed by precipitation using saturated aqueous  $\text{NaClO}_4$  solution. The complexes have been purified by column chromatography on a neutral alumina column (Experimental).

The complexes have been characterised by their satisfactory microanalytical data, molar conductivity and mass spectrometry (Fig. S1† and Experimental). The IR spectrum as KBr disc of **[1]** $\text{ClO}_4$  or **[2]** $\text{ClO}_4$  displays  $\nu(\text{ClO}_4)$  vibrations around  $1100\text{ cm}^{-1}$  and  $625\text{ cm}^{-1}$ ,<sup>10</sup> however, NH vibration of coordinated  $\text{HL}_1$  or  $\text{HL}_2$  has not been clearly resolved primarily due to the appearance of a broad OH vibration around  $3400\text{ cm}^{-1}$ .

The crystal structures of **[1]** $\text{ClO}_4$  and **[2]** $\text{ClO}_4$  are shown in Figs. 1, 2 and selected crystallographic and bond parameters are set in Tables 1, 2 and S1, S2†, respectively. The crystal structure establishes that the ligand  $\text{HL}_1$  or  $\text{HL}_2$  binds to the metal ion by its neutral N donor leaving the free NH proton accessible for further chemical reactivity (see later). The distorted octahedral geometry around the osmium ion in **[1]** $\text{ClO}_4$ /**[2]** $\text{ClO}_4$  has been corroborated by the smaller *trans* angles,  $\text{N1-Os1-N5} = 174.2(3)^\circ/177.3(3)^\circ$ ,  $\text{N3-Os1-N6} = 176.0(3)^\circ/177.7(2)^\circ$ ,  $\text{N4-Os1-Cl1} = 174.4(2)^\circ/173.70(19)^\circ$  and bite angles  $\text{N3-Os1-N4} = 78.7(3)^\circ/78.0(2)^\circ$ ,  $\text{N5-Os1-N6} = 79.2(3)^\circ/78.3(2)^\circ$ ,  $\text{N1-Os1-Cl1} = 90.0(2)^\circ/87.66(17)^\circ$ . The average  $\text{Os}^{\text{II}}\text{-N}(\text{bpy})$ ,<sup>7f-g,11</sup>  $\text{Os}^{\text{II}}\text{-N}(\text{HL})$ <sup>8b,12</sup> and  $\text{Os}^{\text{II}}\text{-Cl}$ <sup>8b,12a-b,13</sup> bond lengths in **[1]** $\text{ClO}_4$ /**[2]** $\text{ClO}_4$  of  $2.043(7)/2.039(7)\text{ \AA}$ ,

2.106(7)/2.104(6) Å and 2.430(2)/2.407(2) Å, respectively, match well with the reported corresponding distances in analogous complexes.

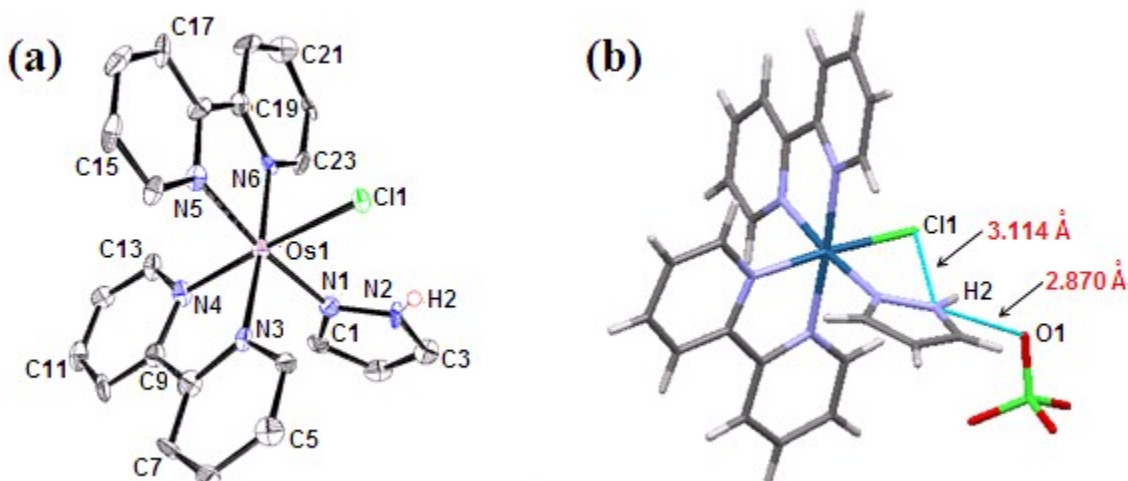


**Fig. 1** (a) ORTEP diagram of the cationic part of [1]ClO<sub>4</sub>. Ellipsoids are drawn at the 40% probability level. Hydrogen atoms (C-H) are omitted for clarity. (b) Perspective view showing the intramolecular N-H...Cl and intermolecular N-H...O hydrogen bonding interactions.

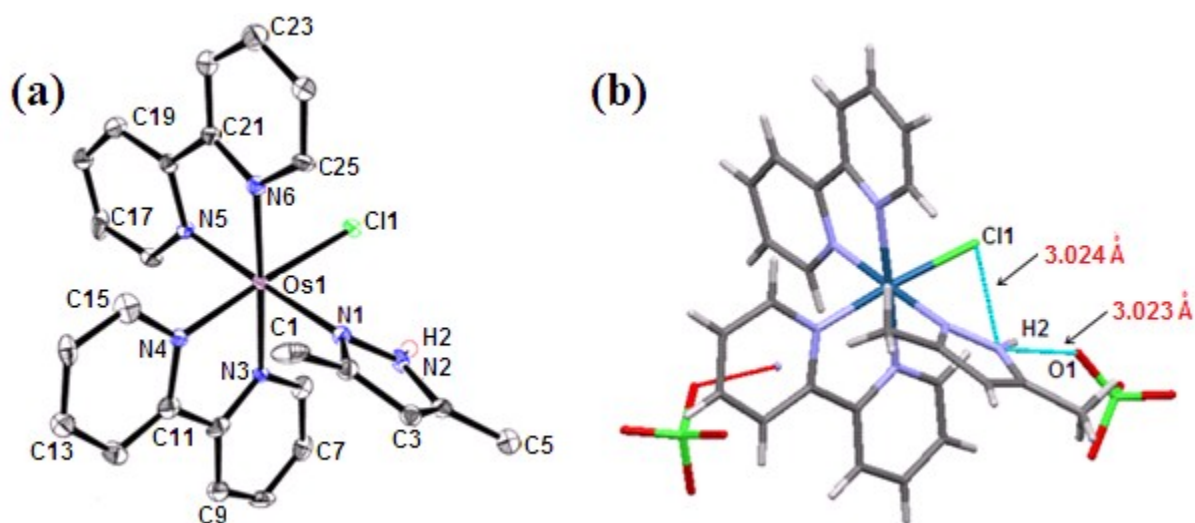


**Fig. 2** (a) ORTEP diagram of the cationic part of [2]ClO<sub>4</sub>. Ellipsoids are drawn at the 40% probability level. Hydrogen atoms (C-H) are omitted for clarity. (b) Perspective view showing the intramolecular N-H...Cl and intermolecular N-H...O hydrogen bonding interactions.

**Table 1** Selected crystallographic parameters of [1]ClO<sub>4</sub> and [2]ClO<sub>4</sub>

Compound	[1]ClO <sub>4</sub>	[2]ClO <sub>4</sub>
Formula	C <sub>23</sub> H <sub>20</sub> N <sub>6</sub> O <sub>4</sub> Cl <sub>2</sub> Os	C <sub>25</sub> H <sub>24</sub> N <sub>6</sub> O <sub>4</sub> Cl <sub>2</sub> Os
<i>M<sub>r</sub></i>	705.55	733.60
Radiation	MoK $\alpha$	MoK $\alpha$
Crystal system	orthorhombic	Monoclinic
Space group	<i>Pbca</i>	<i>P</i> <sub>1</sub> 2 <sub>1</sub> / <i>n</i> <sub>1</sub>
<i>a</i> / $\text{\AA}$	26.520(8)	15.017(8)
<i>b</i> / $\text{\AA}$	13.627(4)	11.932(5)
<i>c</i> / $\text{\AA}$	13.432(4)	15.605(8)
$\alpha$ (°)	90	90
$\beta$ (°)	90	113.401(6)
$\gamma$ (°)	90	90
<i>V</i> / $\text{\AA}^3$	4854(3)	2566(2)
<i>Z</i>	8	4
$\mu$ /mm <sup>-1</sup>	5.518	5.223
<i>T</i> /K	100(2)	100(2)
$\rho_{\text{calcd}}$ /g cm <sup>-3</sup>	1.931	1.899
F(000)	2736	1432
$\theta$ range(°)	3.073 to 25.242	3.139 to 25.00
Data/ restraints/ parameters	4253/0/325	4507/78/345
<i>R</i> <sub>1</sub> , <i>wR</i> <sub>2</sub> [ <i>I</i> > 2 $\sigma$ ( <i>I</i> )]	0.0582, 0.0904	0.0499, 0.0985
<i>R</i> <sub>1</sub> , <i>wR</i> <sub>2</sub> (all data)	0.0656, 0.0931	0.0640, 0.1048
GOF on <i>F</i> <sup>2</sup>	1.246	1.133
Largest diff. peak per hole /e $\text{\AA}^{-3}$	0.949/-0.945	1.631/-1.463



**Table 2** Experimental and DFT calculated selected bond distances (Å) of [1]ClO<sub>4</sub> and [2]ClO<sub>4</sub>

Bond distances (Å)	[1]ClO <sub>4</sub>		[2]ClO <sub>4</sub>	
	X-ray	DFT	X-ray	DFT
Os1-N1	2.106(7)	2.139	2.104(6)	2.165
Os1-N3	2.060(7)	2.087	2.058(7)	2.088
Os1-N4	2.024(7)	2.054	2.020(6)	2.051
Os1-N5	2.044(7)	2.065	2.035(6)	2.066
Os1-N6	2.045(7)	2.077	2.044(7)	2.076
Os1-Cl1	2.430(2)	2.481	2.407(2)	2.486
N1-C1	1.333(10)	1.343	-	-
N1-C2	-	-	1.341(9)	1.351
C1-C2	1.401(12)	1.403	1.504(10)	1.497
C2-C3	1.368(13)	1.386	1.392(10)	1.407
N2-C3	1.353(10)	1.348	-	-
N1-N2	1.342(9)	1.351	1.374(8)	1.361
N2-C4	-	-	1.335(9)	1.350
C3-C4	-	-	1.361(10)	1.387
C4-C5	-	-	1.496(10)	1.495
N2-Cl1	3.114(7)	3.050	3.153(6)	3.032
N2-O1	2.870(10)	-	3.024(8)	-

The appreciably longer Os<sup>II</sup>-N(HL) distance with respect to the Os<sup>II</sup>-N(bpy) distance in [1]ClO<sub>4</sub> or [2]ClO<sub>4</sub> is a reflection of the weak  $\pi$ -accepting feature of HL as compared to bpy.<sup>14</sup> The  $\pi$ -donating ability of Cl<sup>-</sup> has resulted in the shortest Os<sup>II</sup>-N4(bpy) distance (N4 *trans* to Cl<sup>-</sup>) due to the enhanced back bonding effect as compared to the rest of the Os<sup>II</sup>-N(bpy) distances.

The crystal structure of [1]ClO<sub>4</sub> or [2]ClO<sub>4</sub> also confirms the presence of intramolecular as well as intermolecular hydrogen bonding interactions.<sup>12a,15</sup> The intramolecular hydrogen bonding in [1]ClO<sub>4</sub> or [2]ClO<sub>4</sub> takes place between the free NH protons associated with HL and the equatorially positioned Cl<sup>-</sup> with the donor acceptor distance/angle, N2-Cl1/N2-H2...Cl1 of 3.112 Å/123.8<sup>o</sup> or 3.153 Å/114.9<sup>o</sup>, respectively. The intermolecular hydrogen bonding in [1]ClO<sub>4</sub> involves NH proton of the coordinated HL<sub>1</sub> ligand and one of the oxygen atoms (O1) of the

perchlorate counter anion in the asymmetric unit with N2...O1 distance and N2-H2...O1 angle of 2.870 Å and 136.5°, respectively. However, the same in [2]ClO<sub>4</sub> is associated with the NH proton of HL<sub>2</sub> in one asymmetric unit and one of the oxygen atoms (O1) of perchlorate in the nearby asymmetric unit which results in N2-O1 distance of 3.023 Å and N2-H2...O1 angle of 155.9°.

<sup>1</sup>H-NMR spectrum of the diamagnetic [1]ClO<sub>4</sub> in (CD<sub>3</sub>)<sub>2</sub>SO exhibits partially overlapping 16 bpy and 3 CH proton resonances for HL<sub>1</sub> in the chemical shift region  $\delta$ , 6-10 ppm in addition to one NH signal of HL<sub>1</sub> at  $\delta$ , 12.83 ppm (Fig. 3 and Experimental). Though two CH protons of HL<sub>1</sub> are clearly observable at  $\delta$ , 6.79 ppm and 6.29 ppm, the third CH proton is being merged with the bpy resonance at  $\delta$ , 7.08 ppm. The <sup>1</sup>H-NMR of [2]ClO<sub>4</sub> in (CD<sub>3</sub>)<sub>2</sub>SO displays 16 partially overlapping bpy proton resonances in the chemical shift region of  $\delta$ , 6.5-10 ppm and

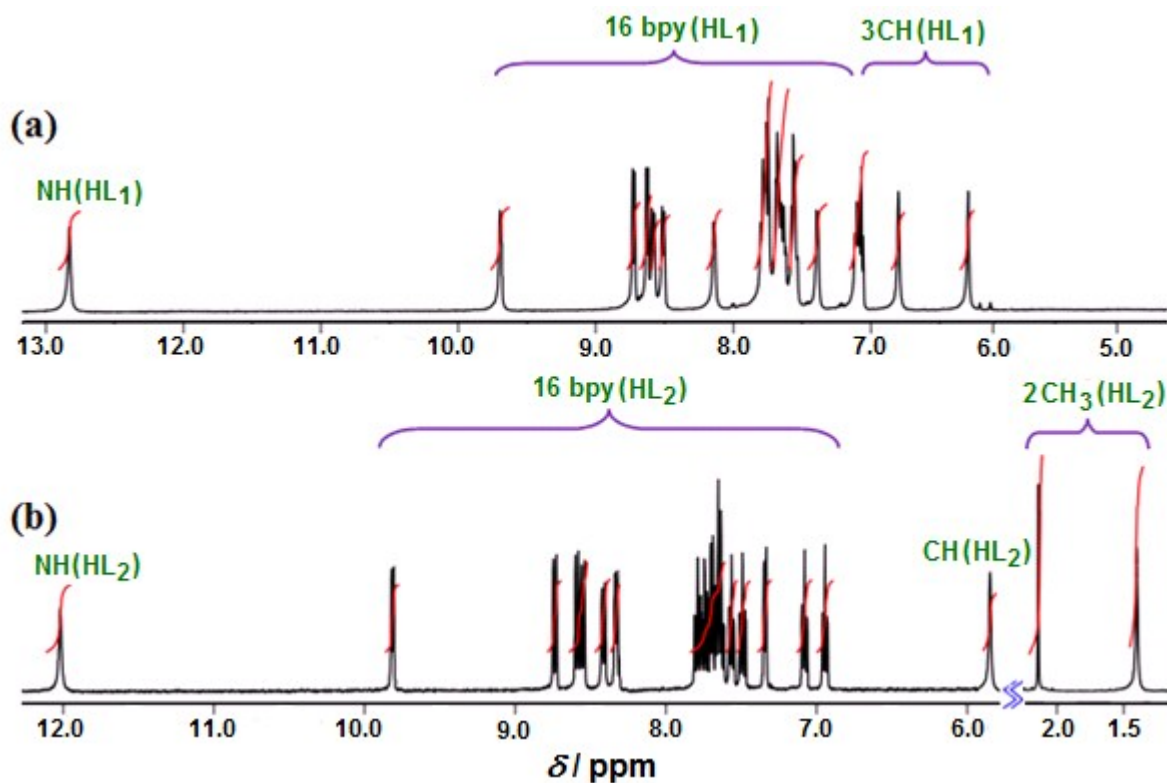


**Fig. 3** <sup>1</sup>H-NMR spectra of (a) [1]ClO<sub>4</sub> and (b) [2]ClO<sub>4</sub> in (CD<sub>3</sub>)<sub>2</sub>SO.

three singlets corresponding to CH proton and 2CH<sub>3</sub> groups of HL<sub>2</sub> at  $\delta$ , 5.84 and 2.18, 1.29 ppm, respectively. The impact of the two electron donating CH<sub>3</sub> groups of HL<sub>2</sub> in **2**<sup>+</sup> in relation to HL<sub>1</sub> in **1**<sup>+</sup> has been reflected in the upfield shifted less acidic NH proton resonance for the former ( $\delta$ , 12.01 ppm) as compared to the latter ( $\delta$ , 12.83 ppm). Furthermore, the presence of intramolecular N-H $\cdots$ Cl and intermolecular N-H $\cdots$ O hydrogen bonding interactions between the NH proton of HL and Cl/oxygen atom of ClO<sub>4</sub><sup>-</sup> counter anion, respectively, in both [**1**]ClO<sub>4</sub> and [**2**]ClO<sub>4</sub> as revealed by their crystal structures (Figs. 1, 2) causes the NH proton of the complexes to appear at the down field region<sup>16</sup> as compared to that of the free pyrazole moiety ( $\delta$ , 11.90 ppm).

### Spectroelectrochemical features

The complexes **1**<sup>+</sup> and **2**<sup>+</sup> display reversible one oxidation (Ox1) and one reduction (Red1) processes with  $E_{298}^0, V$  at  $\sim 0.30$  V and  $\sim -1.70$  V, respectively in CH<sub>3</sub>CN *versus* SCE (Fig. 4, Table 3). The cathodic shift of 40 mV of Ox1 has taken place while moving from **1**<sup>+</sup> to **2**<sup>+</sup> due to

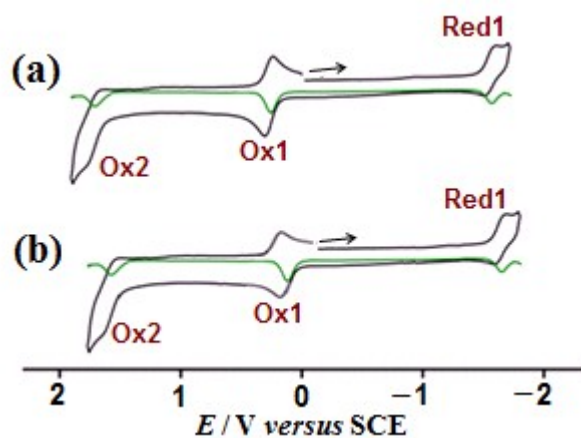


**Fig. 4** Cyclic (black) and differential pulse (green) voltammograms in CH<sub>3</sub>CN/0.1 M NEt<sub>4</sub><sup>+</sup>ClO<sub>4</sub><sup>-</sup> for (a) [**1**]ClO<sub>4</sub> and (b) [**2**]ClO<sub>4</sub>.

**Table 3** Electrochemical data<sup>a</sup>

Complex	$E^{\circ}_{298} / V (\Delta E_p / mV)^b$			Reference
	Ox2	Ox1	Red1	
$[(bpy)_2Os^{II}(HL_1)Cl]^+$	1.70(100)	0.32(60)	-1.69(90)	This work
$[(bpy)_2Os^{II}(HL_2)Cl]^+$	1.57(110)	0.28(60)	-1.71(100)	This work
$[(bpy)_2Ru^{II}(HL_1)Cl]^+$	-	0.81	-	17
$[(bpy)_2Ru^{II}(HL_2)Cl]^+$	-	0.79	-	17

<sup>a</sup>From cyclic voltammetry in CH<sub>3</sub>CN/0.1 M Et<sub>4</sub>NClO<sub>4</sub> at 100 mV s<sup>-1</sup>.

<sup>b</sup>Potentials in V *versus* SCE; peak potential differences  $\Delta E_p$  in parentheses.

the impact of electronic donating two CH<sub>3</sub> groups in the framework of HL<sub>2</sub>. **1**<sup>+</sup> or **2**<sup>+</sup> also exhibits an irreversible second oxidation (Ox2) at around 1.6 V.

The primary involvements of Os (Os<sup>II</sup>/Os<sup>III</sup> (Ox1) and Os<sup>III</sup>→Os<sup>IV</sup> (Ox2) and bpy (Red1) based orbitals in the redox processes of **1**<sup>n</sup> or **2**<sup>n</sup> have been realised by the DFT calculated MO compositions (Tables S3-S11†) and Mulliken spin density distributions at the paramagnetic intermediates (Fig. S2†, Table S12†). The partial contribution of HL/Cl in the MOs and spin distributions in **1**<sup>n</sup> or **2**<sup>n</sup> can be attributed to the effect of metal-ligand covalency.<sup>14a-b,18</sup> The electrochemically generated paramagnetic **1**<sup>2+</sup> or **2**<sup>2+</sup> (*S*=1/2) has however failed to show the expected EPR signal even at 77 K, due to the rapid relaxation process (~10<sup>-8</sup> s) *via* the strong spin orbit coupling effect of heavier Os<sup>III</sup> ion ( $\lambda=3000$  cm<sup>-1</sup>).<sup>19</sup>

The significantly lower Os<sup>II</sup>/Os<sup>III</sup> potential of **1**<sup>+</sup> or **2**<sup>+</sup> as compared to that of the reported analogous [Ru<sup>II</sup>(bpy)<sub>2</sub>(HL)]<sup>+</sup> (0.8 V, Table 3) implies the relatively higher stability of the Os(III) over the Ru(III) state primarily due to the stronger  $\pi$ -donor feature of Os(II).<sup>7g,14a,20</sup>

The change in electronic spectral profiles of **1**<sup>+</sup> and **2**<sup>+</sup> on reversible oxidation to **1**<sup>2+</sup> and **2**<sup>2+</sup>, respectively, has been shown in Fig. 5 and Table S13†. **1**<sup>+</sup> and **2**<sup>+</sup> exhibit similar spectral profile

with multiple bands in the UV-vis region in  $\text{CH}_3\text{CN}$ .<sup>7g,14a,19b,21</sup> The origin of transitions has been evaluated by TD-DFT calculations. The moderately intense lowest energy bands at 724 nm and 734 nm for  $\mathbf{1}^+$  and  $\mathbf{2}^+$  are predicted to be originated *via* the  $(d\pi)\text{Os}/(\pi)\text{Cl}\rightarrow(\pi^*)\text{bpy}$  and  $(d\pi)\text{Os}/(\pi)\text{bpy}\rightarrow(\pi^*)\text{bpy}$  derived MLLCT (metal/ligand to ligand charge transfer) transitions, respectively. The other two intense visible bands at around 520 nm and 430 nm for  $\mathbf{1}^+$  or  $\mathbf{2}^+$  are however of the same origin of  $(d\pi)\text{Os}/(\pi)\text{bpy}\rightarrow(\pi^*)\text{bpy}$ . On oxidation of  $\mathbf{1}^+$  to  $\mathbf{1}^{2+}$  or  $\mathbf{2}^+$  to  $\mathbf{2}^{2+}$ , the lowest energy band around 700 nm of  $\mathbf{1}^+/\mathbf{2}^+$  disappears completely and the visible bands of  $\mathbf{1}^+/\mathbf{2}^+$  around 500 nm undergo slight blue shifting with the significant reduction in intensity, which are

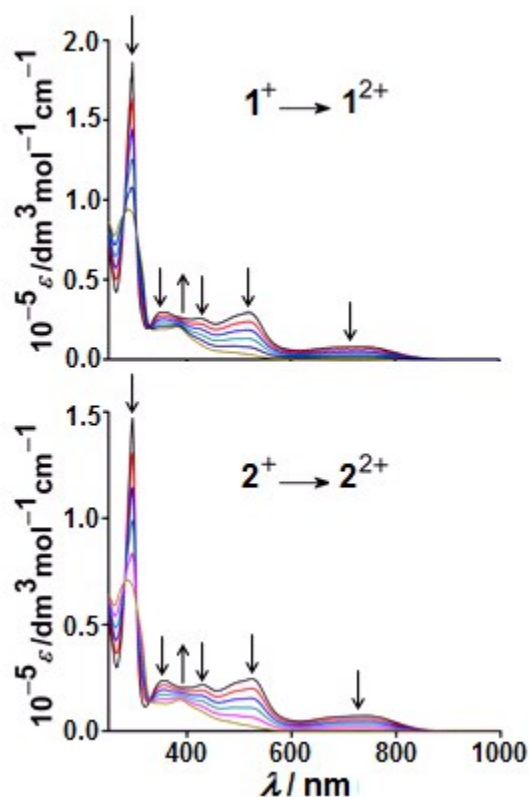


**Fig. 5** Spectroelectrochemical plots for  $\mathbf{1}^+ \rightarrow \mathbf{1}^{2+}$  and  $\mathbf{2}^+ \rightarrow \mathbf{2}^{2+}$  in  $\text{CH}_3\text{CN}$ .

assigned to  $(\pi)\text{HL}/(\pi)\text{bpy}\rightarrow(d\pi)\text{Os}$ ,  $(\pi)\text{bpy}\rightarrow(d\pi)\text{Os}$  and  $(\pi)\text{HL}\rightarrow(d\pi)\text{Os}$  based LLMCT (ligand/ligand to metal charge transfer) and LMCT (ligand to metal charge transfer) transitions.<sup>7g,11</sup>

### Anion binding aspects of $1^+$ and $2^+$

The effectivity of  $1^+$  or  $2^+$  encompassing one hydrogen bonded NH proton in the framework of coordinated HL, as a receptor for the selective interaction with anion(s) has been explored by a series of experimental and DFT calculations.

In this regard, the initial assessment has been made by monitoring the change in colour of  $1^+$  and  $2^+$  on addition of tetrabutylammonium salts of  $F^-$ ,  $Cl^-$ ,  $Br^-$ ,  $I^-$ ,  $OAc^-$ ,  $SCN^-$ ,  $NO_3^-$ ,  $HSO_4^-$ ,  $H_2PO_4^-$ . The introduction of  $F^-/OAc^-$  and  $F^-$  (two equivalents) to the acetonitrile solution of  $1^+$  and  $2^+$ , respectively, has marked a distinct change in colour from brown to violet. However, the colour of  $1^+$  and  $2^+$  remains unaltered even up to the addition of 8 equivalents of  $Cl^-$ ,  $Br^-$ ,  $I^-$ ,  $SCN^-$ ,  $NO_3^-$ ,  $HSO_4^-$  and  $H_2PO_4^-$  (Fig. S3†). The colorimetric experiment thus extends an immediate impression of varying selectivity patterns of  $1^+$  and  $2^+$  towards the tested set of anions which indeed has prompted us to cross examine the anion selectivity features by the following spectroscopic, ITC (Isothermal Titration Calorimetry) and electrochemical techniques.

In agreement to the colorimetric experiment in Fig. S3†, the spectral profile of  $1^+$  or  $2^+$  has failed to change on addition of up to 8 equivalents of  $Cl^-$ ,  $Br^-$ ,  $I^-$ ,  $NO_3^-$ ,  $SCN^-$ ,  $H_2PO_4^-$  and  $HSO_4^-$  (Fig. 6). However, the gradual additions of  $F^-/OAc^-$  and  $F^-$  up to 2 equivalents in  $1^+$  and  $2^+$  have established the shift of MLCT bands at 520 nm to 545 nm/520 nm to 540 nm and 524 nm to 543 nm, respectively, with a sharp change in colour from brown to violet and no further change in band position or intensity is observed thereafter (up to 8 equivalents (Fig. 6)), implying the selectivity of  $F^-/OAc^-$  for the former and  $F^-$  selectivity for the latter. The relatively lower acidity of the NH proton of  $2^+$  ( $pK_a$  of  $1^+$ : ~12.3;  $pK_a$  of  $2^+$  > 13.0 (beyond the scope of instrumental detection, Fig. S4†) due to the impact of electron releasing two methyl groups in the framework of  $HL_2$  can account for this observed exclusive selectivity of  $2^+$  for  $F^-$  in contrast to

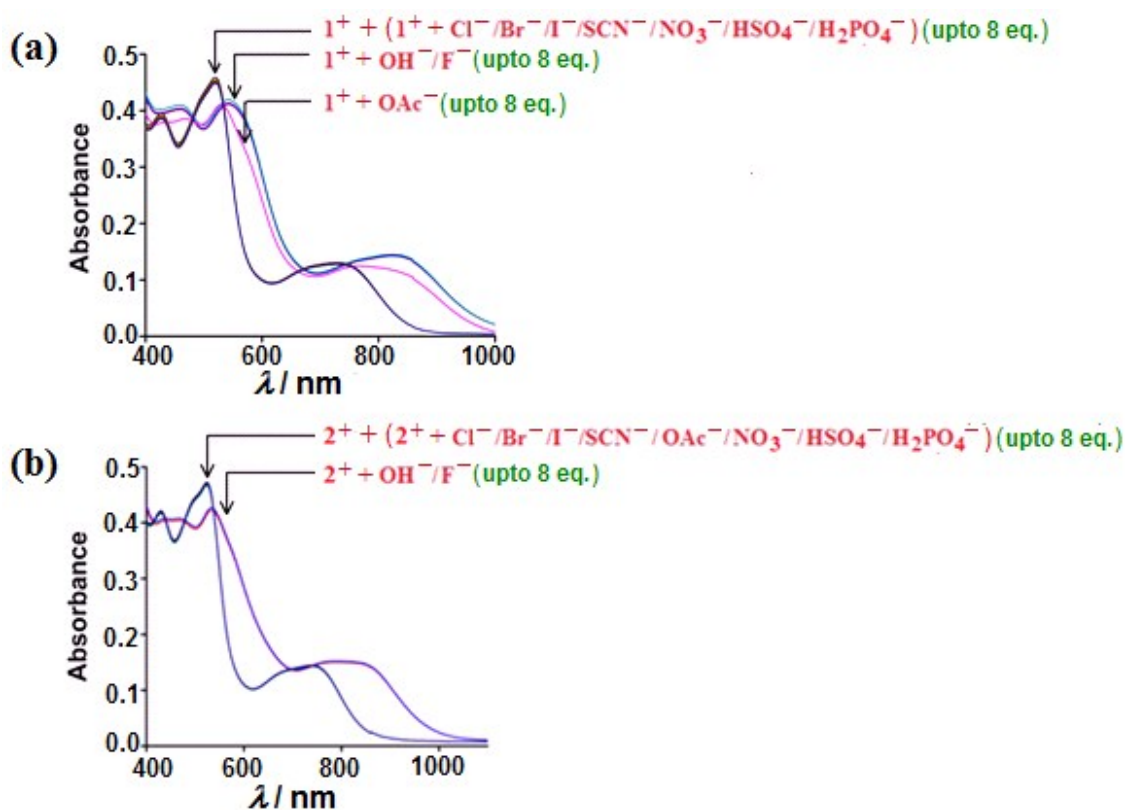


**Fig. 6** UV-vis spectral changes in  $\text{CH}_3\text{CN}$  on addition of eight equivalents of the TBA salt of anions in (a)  $1^+$  and (b)  $2^+$  ( $5 \times 10^{-5} \text{ mol dm}^{-3}$ ).

$\text{F}^-$  and  $\text{OAc}^-$  for  $1^+$ . The deprotonation of HL in  $1^+$  or  $2^+$  via the selective interaction with  $\text{F}^-$  or  $\text{OAc}^-$  has been corroborated by the identical spectral changes in presence of one equivalent stronger base  $\text{OH}^-$  (Fig. 7). The deprotonated **1** and **2** can quantitatively be reconverted to  $1^+$  and  $2^+$ , respectively, in the presence of  $\text{H}_2\text{O}$  as a proton source.

The sequential transformation of  $1^+/2^+$  to the deprotonated state of **1/2** in the presence of  $\text{F}^-$  proceeds through clean isosbestic points (Figs. 7 and S5<sup>†</sup>). The observed spectral saturation with two equivalents of  $\text{F}^-$  suggests 1:2 stoichiometry between the receptor and the interacting anion.<sup>1n,2d,4d,22</sup> However, the requirement of excess equivalents of anion (2 equivalents) for the monodeprotonation process can be attributed to the fact of the weak acidic feature of the NH proton due to its strong intramolecular and intermolecular hydrogen bonding interactions



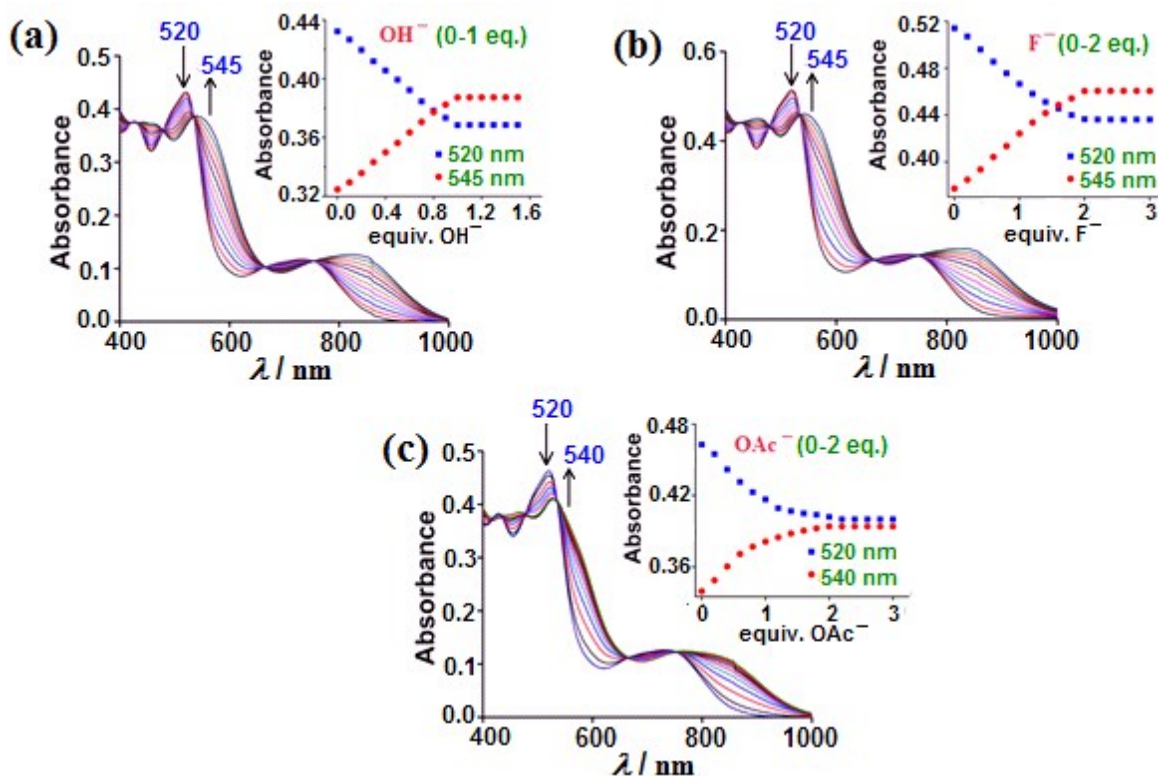


**Fig. 7** UV-vis spectral changes of  $1^+$  ( $5 \times 10^{-5} \text{ mol dm}^{-3}$ ) in  $\text{CH}_3\text{CN}$  on gradual additions of (a)  $\text{OH}^-$ , (b)  $\text{F}^-$  and (c)  $\text{OAc}^-$ . The inset shows the changes in absorbances at 520 nm, 545 nm for  $\text{OH}^-$  and  $\text{F}^-$ ; 520 nm and 540 nm for  $\text{OAc}^-$  as a function of the equivalents of respective anions.

with the equatorially placed  $\text{Cl}^-$  ligand and perchlorate anion, respectively, as evidenced by the crystal structures of  $[1]\text{ClO}_4$  and  $[2]\text{ClO}_4$  (Figs. 1, 2).

The interaction profile of  $1^+$  and  $2^+$  with  $\text{F}^-$  was further investigated by  $^1\text{H-NMR}$  and  $^{19}\text{F-NMR}$  titration in  $(\text{CD}_3)_2\text{SO}$ . The gradual addition of TBAF up to one equivalent (Figs. 8 and S6†) to the solution of  $1^+$  or  $2^+$ , results in broadening of the NH proton signal at  $\delta$ , 12.83 ppm ( $1^+$ ) or 12.01 ppm ( $2^+$ ) followed by its disappearance, possibly due to initial hydrogen bonding interaction with the anion,<sup>4b,d,23</sup> ultimately causing proton abstraction. Moreover, the incremental addition of the anion, up to two equivalents lead to the emergence of a new broad signal (triplet) at around  $\delta$ , 16 ppm corresponding to  $\text{HF}_2^-$ .<sup>24</sup> The effect of anion (up to two equivalents) assisted deprotonation



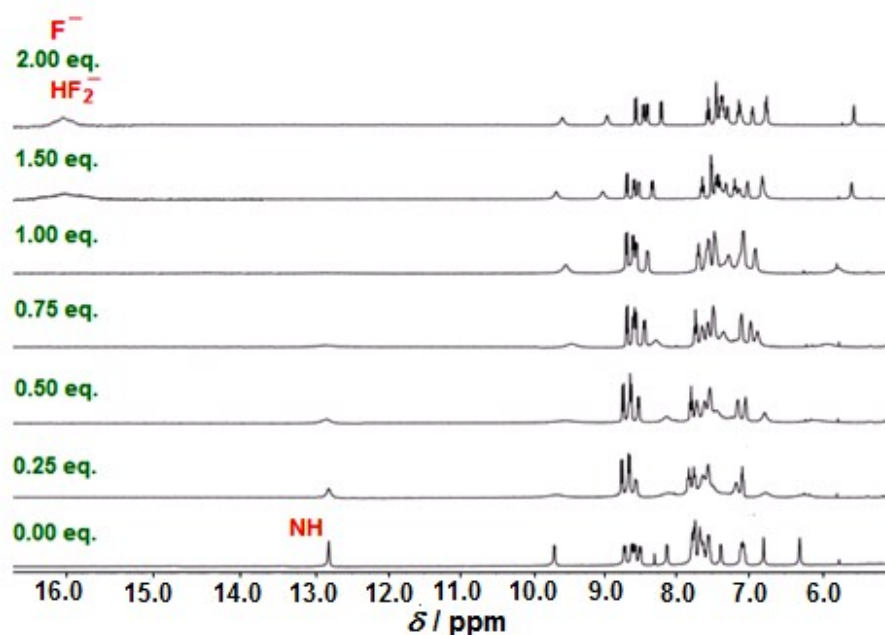


**Fig. 8**  $^1\text{H-NMR}$  titration of  $\mathbf{1}^+$  in  $(\text{CD}_3)_2\text{SO}$  in presence of TBA salt of  $\text{F}^-$  ion (0-2 equivalents).

of  $\mathbf{1}^+$  or  $\mathbf{2}^+$  has also been reflected in the upfield shifted CH proton singlets associated with the coordinated HL along with shifting of the bpy proton resonances. Similar  $^1\text{H-NMR}$  spectral feature has also been obtained on interaction of  $\text{OAc}^-$  with  $\mathbf{1}^+$  (Fig. S7†), although it fails to alter the  $^1\text{H-NMR}$  of  $\mathbf{2}^+$ .

Furthermore,  $^{19}\text{F-NMR}$  of TBAF was recorded which exhibits a characteristic peak at  $\delta$ ,  $-106.72$  ppm in addition to a small peak for  $\text{HF}_2^-$  at  $\delta$ ,  $-144.94$  ppm due to the effect of slight moisture content.<sup>25</sup> This signal for TBAF completely disappears on addition of one equivalent of  $\mathbf{1}^+$  or  $\mathbf{2}^+$ , with a parallel effect of intensity enhancement of  $\text{HF}_2^-$  peak at  $-144.94$  ppm (Fig. S8†), which possibly justifies the initial  $\text{N-H}\cdots\text{F}$  hydrogen bonding interaction, followed by deprotonation and subsequent formation of  $\text{HF}_2^-$ .

In addition, ITC (Isothermal Titration Calorimetry) has also been performed to establish the receptor-anion interaction in terms of relevant thermodynamic parameters of the reaction involving the association constant ( $K$ ), enthalpy ( $\Delta H^\circ$ ), entropy ( $\Delta S^\circ$ ) and stoichiometry ( $N$ ) in a

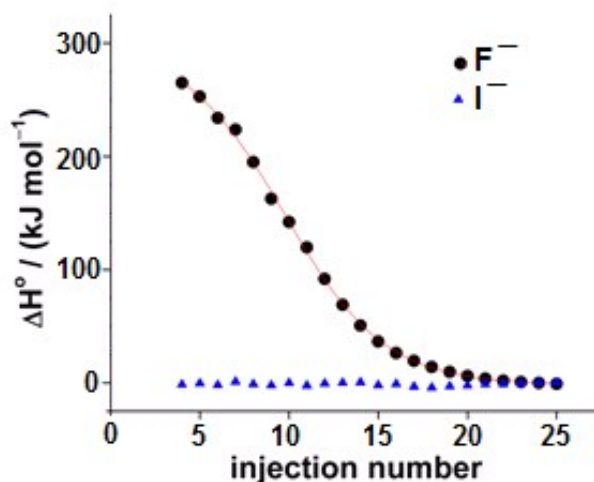
single experiment.<sup>25b,26</sup> As a representative example, we have employed this experiment to ascertain the observed selectivity of  $2^+$  towards  $F^-$  ion *versus* the tested non-interacting anion such as  $I^-$ .

Fig. 9, refers to the integrated heat profile accompanying the titration of  $F^-$  and  $I^-$  ions with  $2^+$  at  $T = 298.15$  K. The data fitted well with the sequential two binding sites model, showing complete saturation at the end of the titrations. The total heat ( $Q$ ) produced or absorbed in the active cell volume ( $V_o$ ) (relative to zero for the blank) at fractional saturation  $\Theta$  after the  $i^{\text{th}}$  injection is given in eqn (1), where,  $C_t$  is the total concentration of  $2^+$  and  $\Delta H^0$  is the molar heat of binding. The enthalpy change ( $\Delta H_i$ ) from the  $i^{\text{th}}$  injection with a volume  $dV_i$  is then derived by the eqn (2).<sup>27</sup>

$$Q = \Theta C_t \Delta H^0 V_o \quad (1)$$

$$\Delta H_i = Q_i + \frac{dV_i}{V_o} \left[ \frac{Q(i) + Q(i-1)}{2} \right] - Q(i-1) \quad (2)$$

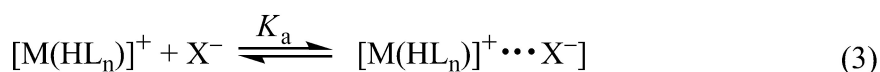
As seen in Fig. 9, the interaction of  $F^-$  with  $2^+$  follows a typical sigmoidal binding pattern, leading to a saturation level. The recognition of  $F^-$  by  $2^+$  is marked by an exothermic event ( $\Delta H_1^0 = -56.7 \pm 0.4$  kJ mol<sup>-1</sup>) followed by an endothermic event ( $\Delta H_2^0 = 332.0 \pm 2.5$  kJ mol<sup>-1</sup>), as reflected by the enthalpies of binding obtained by the analysis of the data according to sequential two binding sites model. The estimated binding constant values are,  $K_1 = (2.28 \pm 0.18) \times 10^4$  M<sup>-1</sup> and  $K_2 = (2.95 \pm 0.30) \times 10^5$  M<sup>-1</sup>. It is further observed that these two binding events are associated with an unfavourable entropic effect ( $\Delta S_1^0 = -0.11 \pm 0.02$  kJ K<sup>-1</sup> mol<sup>-1</sup>) followed by a favourable contribution ( $\Delta S_2^0 = 1.22 \pm 0.08$  kJ K<sup>-1</sup> mol<sup>-1</sup>). The first binding event with  $\Delta G_1^0 = -24.80 \pm 0.20$  kJ mol<sup>-1</sup> involves polar interactions due to hydrogen bond formation between the receptor and the anion, since such interactions are associated with exothermic heat effect<sup>28</sup>



**Fig. 9** Integrated isothermal titration calorimetric heat profile for the titration of  $F^-$  and  $I^-$  with  $2^+$  at  $T = 298.15$  K.

followed by the second binding event with  $\Delta G_2^\circ = -25.51 \pm 0.25$  kJ mol $^{-1}$  which has an endothermic enthalpy contribution involving the cleavage of the hydrogen bonded intermediate to **2** and forming  $HF_2^-$ , as stated below in eqn (3) and (4). On the other hand, the consecutive injections of  $I^-$  into the acetonitrile solution of  $2^+$  did not result in any appreciable heat change, suggesting the absence of recognition. The isothermal calorimetric measurements (Fig. 9) thus revealing the integrated heat profile accompanying the titration of  $2^+$  with  $F^-$  or  $I^-$ , are in agreement with the preceding experimental observations.

The experiments thus mentioned above collectively suggest a two step process between the receptor and anion, i.e. the association of receptor-anion, as also evident by the *in situ* mass experiment (Fig. S9 $\dagger$ ), leading to the eventual deprotonation. This two step process<sup>2d,22a,29</sup> can be expressed as:



The minor change in the UV-vis spectra on addition of one equivalent of anion has restrained us to calculate  $\log K_a$  (association constant) from the spectrophotometric titration. However,  $\log K_d$  (dissociation constant) values have been calculated to be 6.57/5.91 (in case of  $\mathbf{1}^+$  for  $\text{F}^-/\text{OAc}^-$ ) and 6.17 (in case of  $\mathbf{2}^+$  for  $\text{F}^-$ ), as shown in Fig. S10†.

In general, the selective anion recognition features of  $\mathbf{1}^+$  and  $\mathbf{2}^+$  could tentatively be defined in terms of the basicity ( $\text{p}K_a(\text{aq})$ ) of the halogen acids and the oxy-anions:  $\text{HF}$  (3.45) >  $\text{HCl}$ (-7) >  $\text{HBr}$  (-9) >  $\text{HI}$  (-11) and  $\text{HOAc}$  (4.75) >  $\text{H}_3\text{PO}_4$  (2.12) >  $\text{H}_2\text{SO}_4/\text{HSCN}$  (-2) >  $\text{HNO}_3$  (-1.3).<sup>30</sup> However, the observed inertness of  $\mathbf{2}^+$  towards  $\text{OAc}^-$  with even greater  $\text{p}K_a(\text{aq})$  of  $\text{HOAc}$  than that of  $\text{HF}$  implies that the basicity of anion/receptor and the strength of hydrogen bonding interaction collectively control the proton transfer process from the receptor to the anion.<sup>30b</sup>

The stoichiometry of 1:2 between the receptor and anion as established in the preceding sections has also been ascertained by monitoring the change in reversible  $\text{Os}^{\text{II}}/\text{Os}^{\text{III}}$  oxidation(Ox1) process of  $\mathbf{1}^+$  and  $\mathbf{2}^+$  (Fig. 4) as a function of varying equivalents of aforesaid anions in  $\text{CH}_3\text{CN}$  (Fig. 10). The Ox1 potential of  $\mathbf{1}^+$  or  $\mathbf{2}^+$  at 0.32 V or 0.28 V in  $\text{CH}_3\text{CN}$  (Fig. 4) remains unchanged on addition of up to eight equivalents of  $\text{Cl}^-$ ,  $\text{Br}^-$ ,  $\text{I}^-$ ,  $\text{SCN}^-$ ,  $\text{NO}_3^-$ ,  $\text{HSO}_4^-$  and  $\text{H}_2\text{PO}_4^-$ . However, an appreciable decrease in the oxidation potential has selectively been taken place on addition of two equivalents of  $\text{F}^-/\text{OAc}^-$  to  $\mathbf{1}^+$  (-0.07 V) and  $\text{F}^-$  to  $\mathbf{2}^+$  (-0.16 V). The lowering in potential on addition of anion is due to the increase in electron density on the metal centre by the anion mediated deprotonation of the coordinated HL, i.e the effect of the changeover of an weakly  $\pi$ -accepting HL in  $\mathbf{1}^+/\mathbf{2}^+$  to the weakly  $\pi$ -donating  $\text{L}^-$  in  $\mathbf{1}/\mathbf{2}$ .

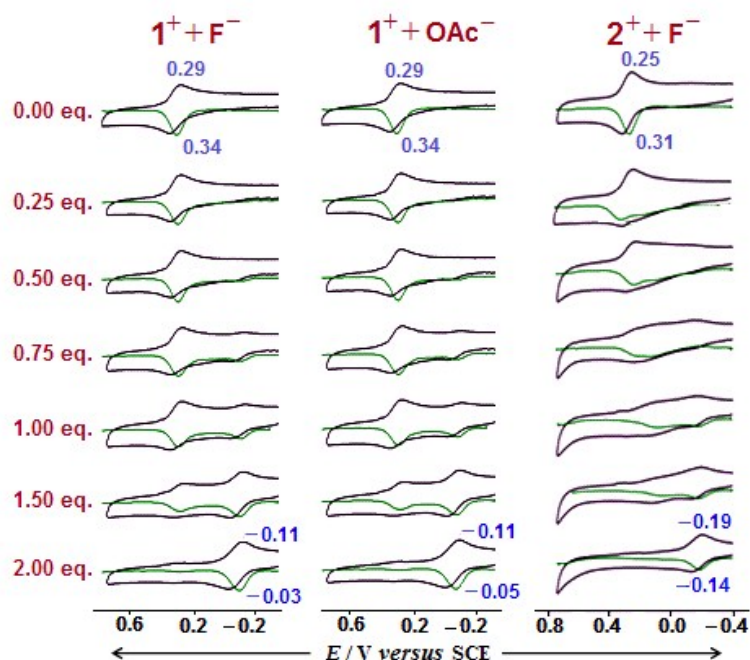


**Fig. 10** Sequential changes in voltammograms (black) and differential pulse voltammograms (green) (reversible oxidation couple (Ox1 in Fig. 4) only) of  $1^+$  and  $2^+$  in  $\text{CH}_3\text{CN}$  ( $5 \times 10^{-5}$  mol  $\text{dm}^{-3}$ ) upon gradual additions of anions.

The DFT (NBO) calculations have been performed to understand the mode of interaction between the receptors ( $1^+/2^+$ ) and the anions ( $X=\text{F}^-/\text{OAc}^-$ ). The lengthening of N(2)-H(2) distance (1.607 Å, 1.589 Å/1.719 Å) in optimised  $\mathbf{A}/\mathbf{A}'/\mathbf{B}$  (i.e.  $1^+/2^+\cdots X^-$ ) as compared to that of 1.022 Å in optimised  $1^+/2^+$  (Figs. S11, S12<sup>†</sup>), along with the shortening of H(2)- $X^-$  distance by 0.984 Å, 0.992 Å/1.017 Å (Table 4) collectively suggest the intermediate hydrogen bonding interaction between the receptor and anion followed by breaking of N(2)-H(2) bond with a concomitant formation of H(2)- $X^-$  bond. The N(2)-H(2)- $X^-$  angles of 167.8°, 163.3°/165.2° and D(donor) $\cdots$ A(acceptor) distances of 2.579 Å, 2.556 Å/2.715 Å in  $\mathbf{A}/\mathbf{A}'/\mathbf{B}$  (Table 4) also corroborate the hydrogen bond mediated deprotonation process.<sup>4</sup> The decrease in natural charge over N(2) and increase in natural charge over H(2) in the optimised structures of  $\mathbf{A}/\mathbf{A}'/\mathbf{B}$  with

**Table 4** DFT calculated structural parameters and NBO charges

Complex	X <sup>-</sup>	d(N2-H2) Å	d(H2...X) Å	α(N2-H2-X) <sup>o</sup>	q <sub>N</sub>	q <sub>H</sub>	q <sub>X</sub>	q <sub>Os</sub>
<b>1<sup>+</sup></b>	-	1.022	-	-	-0.319	0.461	-	0.227
<b>A</b>	F <sup>-</sup>	1.607	0.984	167.8	-0.357	0.549	-0.623	0.258
<b>B</b>	OAc <sup>-</sup>	1.719	1.017	165.2	-0.383	0.522	-0.592	0.274
<b>2<sup>+</sup></b>	-	1.022	-	-	-0.327	0.452	-	0.231
<b>A'</b>	F <sup>-</sup>	1.589	0.992	163.3	-0.362	0.548	-0.624	0.262

respect to **1<sup>+</sup>/2<sup>+</sup>** (Table 4) also endorse the above consideration.<sup>4</sup> The slight increment of the natural charge on Os in **A/A'/B** is a mere reflection of the change in the electronic environment around the metal centre in the presence of anions.

A close look at the DFT optimised structures of [**1<sup>+</sup>...F**] and [**1<sup>+</sup>...OAc**] (Fig. S12<sup>†</sup>) reveals the rotation of the pyrazole plane in **1<sup>+</sup>** while interacting with the OAc<sup>-</sup>. Such rotation of the dimethyl substituted pyrazole might have been restricted in **2<sup>+</sup>** due to the steric reason which possibly can account for its exclusive selectivity towards the F<sup>-</sup> over OAc<sup>-</sup>.

## Conclusions

In conclusion, osmium-coordinated pyrazolyl framework, [(bpy)<sub>2</sub>Os<sup>II</sup>(HL<sub>1</sub>)Cl]<sup>+</sup> [**1**]ClO<sub>4</sub> or [(bpy)<sub>2</sub>Os<sup>II</sup>(HL<sub>2</sub>)Cl]<sup>+</sup> [**2**]ClO<sub>4</sub> (HL<sub>1</sub> = pyrazole, HL<sub>2</sub> = 3,5-dimethylpyrazole) has been designed with the primary objective of exploring its feasibility to function as an efficient receptor for the selective anion recognition process. The structural analysis of [**1**]ClO<sub>4</sub> or [**2**]ClO<sub>4</sub> extends the additional features of intramolecular N-H...Cl and intermolecular N-H...O(ClO<sub>4</sub>) hydrogen bonding interactions, revealing the fact of lesser accessibility of the NH proton of coordinated HL for the possible interaction with the incoming anions as has also been ascertained by its high pK<sub>a</sub> value (**1<sup>+</sup>**: ~12.3, **2<sup>+</sup>**: >13.0). The impact of substituent in the framework of HL (H(**1<sup>+</sup>**) *versus*

Me( $\mathbf{2}^+$ ) on the acidity of the NH protons has in turn made  $\mathbf{2}^+$  exclusively selective for the  $\text{F}^-$  ion, while  $\mathbf{1}^+$  recognises both  $\text{F}^-$  and  $\text{OAc}^-$ .

## Experimental section

### Materials

The metal precursor  $cis-[Os^{II}(bpy)_2Cl_2] \cdot 2H_2O$ <sup>31</sup> was prepared according to the literature procedure. Pyrazole (HL<sub>1</sub>), 3,5-dimethylpyrazole (HL<sub>2</sub>) and tetrabutylammonium salts of F<sup>-</sup>, OH<sup>-</sup>, Cl<sup>-</sup>, Br<sup>-</sup>, I<sup>-</sup>, OAc<sup>-</sup>, SCN<sup>-</sup>, NO<sub>3</sub><sup>-</sup>, HSO<sub>4</sub><sup>-</sup>, H<sub>2</sub>PO<sub>4</sub><sup>-</sup> were obtained from Sigma-Aldrich. All other chemicals and solvents were of reagent grade and used as received. For spectroscopic and electrochemical studies HPLC grade solvents were used.

### Physical measurements

The electrical conductivities of the complexes in CH<sub>3</sub>CN were checked by using an Autoranging conductivity meter (Toshcon Industries, India). <sup>1</sup>H-NMR and <sup>19</sup>F-NMR spectra were recorded using Bruker Avance III 400 and 500 MHz spectrometers. The elemental analyses were carried out on a Thermoquest (EA 1112) micro analyser. Electrospray mass spectra were recorded on a Bruker's Maxis Impact (282001.00081). Cyclic voltammetric and differential pulse voltammetric measurements were performed on a PAR model 273A electrochemistry system. NEt<sub>4</sub><sup>+</sup>ClO<sub>4</sub><sup>-</sup> was used as the electrolyte and the solute concentration was  $\sim 10^{-3}$  mol dm<sup>-3</sup>. A glassy carbon working electrode, a platinum wire auxiliary electrode, and a saturated calomel reference electrode (SCE) were used in a standard three-electrode configuration cell. A platinum wire-gauze working electrode was used for the constant potential coulometry experiment. All electrochemical experiments were carried out under dinitrogen atmosphere at 298 K. The half-wave potential  $E^0$  was set equal to  $0.5(E_{pa} + E_{pc})$ , where  $E_{pa}$  and  $E_{pc}$  are anodic and cathodic cyclic voltammetry peak potentials, respectively. Spectroelectrochemical studies were performed on a BAS SEC2000 spectrometer system. The supporting electrolyte was NEt<sub>4</sub><sup>+</sup>ClO<sub>4</sub><sup>-</sup> and the



solute concentration was  $10^{-5}$  mol dm $^{-3}$ . UV-vis studies were performed on a Perkin-Elmer Lambda 1050 spectrophotometer. FT-IR spectra were taken on a Nicolet spectrophotometer with samples prepared as KBr pellets. Isothermal titration calorimetry (ITC) measurement was performed using NANO ITC, procured from TA instruments, New Castle, USA.

For spectrophotometric titrations, in each step 2  $\mu$ L aliquot of the TBA salt of the respective anions ( $5 \times 10^{-3}$  mol dm $^{-3}$ ) in CH $_3$ CN was added by a micro-syringe in 2 cm $^3$  CH $_3$ CN solution of **1** $^+$  or **2** $^+$  ( $5 \times 10^{-5}$  mol dm $^{-3}$ ) using a quartz cuvette with 1 cm path length. Based on the spectrophotometric titrations,  $\log K_d$  has been calculated using eqn (5)<sup>32</sup> where  $\Delta A$  represents the

$$\Delta A = \frac{\Delta \epsilon [M(HL_n)^+] + 1/K_d + (\Delta \epsilon^2 ([M(HL_n)^+] + [X^-] + 1/K_d)^2 - 4\Delta \epsilon^2 [M(HL_n)^+][X^-])^{1/2}}{2} \quad (5)$$

change in initial absorbance upon each addition of the anions ( $X^- = F^-/OAc^-$ ) in **1** $^+$  or **2** $^+$ .  $[M(HL_n)^+]$  and  $[X^-]$  correspond to their respective concentrations during the spectrophotometric titrations.

The dissociation constant ( $K_d$ ) and the change in molar extinction coefficient ( $\Delta \epsilon$ ) at each concentration of  $F^-/OAc^-$  for **1** $^+$  and  $F^-$  for **2** $^+$  are evaluated by the nonlinear curve fitting procedure. For electrochemical titration, 25  $\mu$ L aliquot of the TBA salt of the respective anions ( $5 \times 10^{-3}$  mol dm $^{-3}$ ) in acetonitrile was added by a micropipette in each step in 20 cm $^3$  acetonitrile solution of **1** $^+$  or **2** $^+$  ( $5 \times 10^{-5}$  mol dm $^{-3}$ ). For isothermal titration calorimetric measurements, the solution of  $F^-$  or  $I^-$  prepared in acetonitrile was titrated into the sample cell in aliquots using a 250  $\mu$ L stirrer-syringe rotating at a speed of 250 rpm. The calorimeter consists of a matched pair of sample and reference cells, each having a volume of 1.0 cm $^3$ , placed in an adiabatic enclosure. The reference cell was filled with acetonitrile and closed with the cap provided with the calorimeter. The sample cell contained the compound **2** $^+$  in acetonitrile. Each experiment consisted of 25 consecutive injections of 10  $\mu$ L of 1 mmol dm $^{-3}$   $F^-/I^-$  solution into 0.01 mmol

$\text{dm}^{-3}$   $2^+$  taken in the cell for the duration of 6 s with 6 min interval between the consecutive injections. This arrangement provided sufficient time for the power signal to reach back the base line after each injection. Heats of dilution were obtained by titrating  $\text{F}^-/\text{I}^-$  or  $2^+$  with the solvent acetonitrile under the identical concentrations as used in the main experiment. The integrated heat profiles were corrected for the observed heats of dilutions.

### Crystallography

Single crystals of  $[\mathbf{1}]\text{ClO}_4$  and  $[\mathbf{2}]\text{ClO}_4$  were grown by slow evaporation of their 1:1 dichloromethane-toluene solution. The X-ray crystal data were collected on RIGAKU SATURN-724+ CCD single crystal X-ray diffractometer. The data were collected by the standard omega scan technique and were scaled and reduced using the CrystalClear-SM Expert software. The structures were solved by direct method using SHELXS-97 and refined by full matrix least-squares with SHELXL2012, refining on  $F^2$ .<sup>33</sup> All non-hydrogen atoms were refined anisotropically. The remaining hydrogen atoms were placed in geometrically constrained positions and refined with isotropic temperature factors, generally  $1.2U_{\text{eq}}$  of their parent atoms. Hydrogen atoms were included in the refinement process as per the riding model. CCDC-1430164 ( $[\mathbf{1}]\text{ClO}_4$ ) and 1430165 ( $[\mathbf{2}]\text{ClO}_4$ ) contain the supplementary crystallographic data for this paper. These data can be obtained free of charge from The Cambridge Crystallographic Data Centre via [www.ccdc.cam.ac.uk/data\\_request/cif](http://www.ccdc.cam.ac.uk/data_request/cif).

### Computational details

Full geometry optimisations were carried out by using the density functional theory method at the (R)B3LYP level for  $1^+$ ,  $2^+$ ,  $\mathbf{A}$ ,  $\mathbf{A}'$ ,  $\mathbf{B}$  and (U)B3LYP level for  $1^{2+}$ ,  $1^{3+}$ ,  $2^{2+}$ ,  $2^{3+}$ ,  $\mathbf{1}$  and  $\mathbf{2}$ .<sup>34</sup> All elements except osmium were assigned the 6-31G\* basis set. The LANL2DZ basis set with

effective core potential was employed for the osmium atom.<sup>35</sup> The vibrational frequency calculations were performed to ensure that the optimised geometries represent the local minima and there are only positive eigen values. All calculations were performed with Gaussian09 program package.<sup>36</sup> Vertical electronic excitations based on (R)B3LYP/(U)B3LYP optimised geometries were computed for **1**<sup>n</sup> (*n* = +2, +1) and **2**<sup>n</sup> (*n* = +2, +1) using the time-dependent density functional theory (TD-DFT) formalism<sup>37</sup> in acetonitrile with the conductor-like polarisable continuum model (CPCM).<sup>38</sup> Natural bond orbital analysis was performed using the NBO 3.1 module of Gaussian 09 on optimised geometries. Chemissian 1.7<sup>39</sup> was used to calculate the fractional contributions of various groups to each molecular orbital. All the calculated structures were visualised with ChemCraft.<sup>40</sup>

### Preparation of complexes

**Synthesis of [Os<sup>II</sup>(bpy)<sub>2</sub>(HL<sub>1</sub>)]ClO<sub>4</sub>, [1]ClO<sub>4</sub> and [Os<sup>II</sup>(bpy)<sub>2</sub>(HL<sub>2</sub>)]ClO<sub>4</sub>, [2]ClO<sub>4</sub>.** The precursor complex *cis*-[Os<sup>II</sup>(bpy)<sub>2</sub>(Cl)<sub>2</sub>] (100 mg, 0.17 mmol) and the ligand HL<sub>1</sub> (24 mg, 0.35 mmol) or HL<sub>2</sub> (33 mg, 0.35 mmol) were taken up in 30 cm<sup>3</sup> of 1:1 ethanol-water and the mixture was refluxed under dinitrogen atmosphere for 48 h. The initial light brown colour of the reaction mixture gradually changed to deep brown. The solvent was then removed under reduced pressure. The residue was moistened with a few drops of CH<sub>3</sub>CN, followed by the addition of saturated aqueous NaClO<sub>4</sub> solution yielding a dark precipitate, which was filtered off, washed thoroughly with ice-cold water to remove the excess NaClO<sub>4</sub> and dried under vacuum. The crude product was purified on a neutral alumina column which led to the elution of the desired complex [1]ClO<sub>4</sub> by CH<sub>3</sub>CN-MeOH (1:2) or [2]ClO<sub>4</sub> by CH<sub>2</sub>Cl<sub>2</sub>-CH<sub>3</sub>CN (2:1). Evaporation of the solvent under reduced pressure yielded the pure complexes.

**[1]ClO<sub>4</sub>**. Yield: 80 mg, 65%. Anal. calcd for C<sub>23</sub>H<sub>20</sub>N<sub>6</sub>O<sub>4</sub>Cl<sub>2</sub>Os: C, 39.15; H, 2.86; N, 11.91; found: C, 39.23; H, 2.79; N, 11.82.  $A_M$  ( $\Omega^{-1} \text{ cm}^2 \text{ M}^{-1}$ ) in acetonitrile at 298 K: 115. ESI-MS(+) in CH<sub>3</sub>CN,  $m/z$ : calcd for {**1**}<sup>+</sup>: 607.096; found: 607.120. <sup>1</sup>H-NMR (500 MHz, DMSO-d<sub>6</sub>):  $\delta$ , (ppm, J(Hz)): 12.83 (s, 1H, NH), 9.69 (d, 1H, 5.1), 8.72 (d, 1H, 8.1), 8.62 (d, 1H, 8.1), 8.58 (d, 1H, 7.9), 8.51 (d, 1H, 8.0), 8.13 (d, 1H, 4.4), 7.77 (m, 3H), 7.65 (m, 3H), 7.55 (m, 2H), 7.38 (d, 1H, 5.2), 7.08 (m, 2H), 6.79 (s, 1H, CH), 6.29 (s, 1H, CH).

**[2]ClO<sub>4</sub>**. Yield: 64 mg, 50%. Anal. calcd for C<sub>25</sub>H<sub>24</sub>N<sub>6</sub>O<sub>4</sub>Cl<sub>2</sub>Os: C, 40.93; H, 3.30; N, 11.46; found: C, 40.72; H, 3.41; N, 11.29.  $A_M$  ( $\Omega^{-1} \text{ cm}^2 \text{ M}^{-1}$ ) in acetonitrile at 298 K: 110. ESI-MS(+) in CH<sub>3</sub>CN,  $m/z$ : calcd for {**2**}<sup>+</sup>: 635.125; found: 635.412. <sup>1</sup>H-NMR (400 MHz, DMSO-d<sub>6</sub>):  $\delta$ , (ppm, J(Hz)): 12.01 (s, 1H, NH), 9.81 (d, 1H, 5.6), 8.74 (d, 1H, 8.1), 8.57 (m, 2H), 8.41 (d, 1H, 8.2), 8.33 (d, 1H, 5.6), 7.71 (m, 5H), 7.55 (m, 1H), 7.48 (m, 1H), 7.34 (d, 1H, 5.5), 7.08 (m, 1H), 6.94 (m 1H), 5.84 (s, 1H, CH), 2.18 (s, 3H, CH<sub>3</sub>), 1.29 (s, 3H, CH<sub>3</sub>).

(**CAUTION!** Perchlorate salts are potentially explosive and should be handled with appropriate care).

## Acknowledgements

Financial support received from the Department of Science and Technology, Council of Scientific and Industrial Research (fellowship to AD and PM), New Delhi, India and IIT Bombay (fellowship to MD), India is gratefully acknowledged.

## References

- 1 (a) E. Bianchi, K. Bowman-James, and E. García-Espana, *Supramolecular Chemistry of Anions*, Wiley Publishing: New York, 1997; (b) P. Gamez, T. J. Mooibroek, S. J. Teat and J. Reedijk, *Acc. Chem. Res.*, 2007, **40**, 435; (c) M. Arunachalam, I. Ravikumar and P. Ghosh, *J. Org. Chem.*, 2008, **73**, 9144; (d) R. Dutzler, E. B. Campbell, M. Cadene, B. T. Chait and R. MacKinnon, *Nature*, 2002, **415**, 287; (e) H. Maeda and H. Ito, *Inorg. Chem.*, 2006, **45**, 8205; (f) P. A. Gale, *Coord. Chem. Rev.*, 2003, **240**, 1; (g) J. L. Sessler, P.A. Gale, W. S. Cho and J. F. Stoddart, *Anion Receptor Chemistry*, Monographs in Supramolecular Chemistry, Ed. Royal Society of Chemistry: Cambridge, U.K. 2006; (h) P. A. Gale, *Coord. Chem. Rev.*, 2006, **250**, 2917; (i) J. L. Sessler and J. M. Davis, *Acc. Chem. Res.*, 2001, **34**, 989; (j) C. Caltagirone and P. A. Gale, *Chem. Soc. Rev.*, 2009, **38**, 520; (k) P. A. Gale, S. E. Garcia-Garrido and J. Garric, *Chem. Soc. Rev.*, 2008, **37**, 151; (l) P. D. Beer and P. A. Gale, *Angew. Chem., Intl. Ed.*, 2001, **40**, 486; (m) V. Amendola and L. Fabbrizzi, *Chem. Commun.*, 2009, 513; (n) X. Peng, Y. Wu, J. Fan, M. Tian and K. Han, *J. Org. Chem.*, 2005, **70**, 10524.
- 2 (a) S. Verma, S. Aute, A. Das and H. N. Ghosh, *J. Phys. Chem. B*, DOI: 10.1021/acs.jpcc.5b09227; (b) C. Suksai and T. Tuntulani, *Chem. Soc. Rev.*, 2003, **32**, 192; (c) V. Amendola, M. Boiocchi, L. Fabbrizzi and A. Palchetti, *Chem. -Eur. J.*, 2005, **11**, 120; (d) V. Amendola, D. E. Gomez, L. Fabbrizzi and M. Licchelli, *Acc. Chem. Res.*, 2006, **39**, 343; (e) R. Martínez-Mañez and F. Sancenón, *Chem. Rev.*, 2003, **103**, 4419.
- 3 (a) K.-C. Chang, S.-S. Sun, M. O. Odago and A. J. Lees, *Coord. Chem. Rev.*, 2015, **284**, 111; (b) P. D. Beer, *Acc. Chem. Res.*, 1998, **31**, 71; (c) P. D. Beer and E. J. Hayes, *Coord. Chem. Rev.*, 2003, **240**, 167.

- 4 (a) J. Wang, F.-Q. Bai, B.-H. Xia, L. Sun and H.-X. Zhang, *J. Phys. Chem. A*, 2011, **115**, 1985; (b) T. Kundu, A. D. Chowdhury, D. De, S. M. Mobin, V. G. Puranik, A. Datta and G. K. Lahiri, *Dalton Trans.*, 2012, **41**, 4484; (c) T. Ghosh and B. G. Maiya, *J. Phys. Chem. A*, 2004, **108**, 11249; (d) M. Sarkar, R. Yellampalli, B. Bhattacharya, R. K. Kanaparthi and A. Samanta, *J. Chem. Sci.*, 2007, **119**, 91; (e) D. W. Kim, J. Kim, J. Hwang, J. K. Park and J. S. Kim, *Bull. Korean Chem. Soc.*, 2012, **33**, 1159.
- 5 (a) S. J. Dickson, S. C. G. Biaginib and J. W. Steed, *Chem. Commun.*, 2007, 4955; (b) S. J. Dickson, M. J. Paterson, C. E. Willans, K. M. Anderson and J. W. Steed, *Chem.-Eur. J.*, 2008, **14**, 7296; (c) J. G. Vos and J. M. Kelly, *Dalton Trans.*, 2006, 4869; (d) S. Derossi, H. Adams and M. D. Ward, *Dalton Trans.*, 2007, 33.
- 6 (a) M. H. V. Huynh, D. M. Dattelbaum and T. J. Meyer, *Coord. Chem. Rev.*, 2005, **249**, 457; (b) F. Szemes, D. Heseck, Z. Chen, S. W. Dent, M. G. B. Drew, A. J. Goulden, A. R. Graydon, A. Grieve, R. J. Mortimer, T. Wear, J. S. Weightman and P. D. Beer, *Inorg. Chem.*, 1996, **35**, 5868; (c) P. D. Beer, S. W. Dent and T. J. Wearb, *J. Chem. Soc., Dalton Trans.*, 1996, 2341; (d) E. Berni, I. Gosse, D. Badocco, P. Pastore, N. Sojic and S. Pinet, *Chem. -Eur. J.*, 2009, **15**, 5145; (e) D. Maity, C. Bhaumik, D. Mondal and S. Baitalik, *Inorg. Chem.*, 2013, **52**, 13941; (f) D. Maity, C. Bhaumik, D. Mondal and S. Baitalik, *Dalton Trans.*, 2014, **43**, 1829.
- 7 (a) P. D. Beer, V. Balzani, C. Salà, M. G. B. Drew, S. W. Dent and M. Maestri, *J. Am. Chem. Soc.*, 1997, **119**, 11864; (b) S. Das, D. Saha, C. Bhaumik, S. Dutta and S. Baitalik, *Dalton Trans.*, 2010, **39**, 4162; (c) J. Lehr, T. Lang, O. A. Blackburn, T. A. Barendt, S. Faulkner, J. J. Davis, P. D. Beer, *Chem. -Eur. J.*, 2013, **19**, 15898; (d) C. Bhaumik, S. Das, D. Saha, S. Dutta and S. Baitalik, *Inorg. Chem.*, 2010, **49**, 5049; (e) D. Saha, S. Das, D.

Maity, S. Dutta and S. Baitalik, *Inorg. Chem.*, 2011, **50**, 46; (f) A. Das, S. M. Mobin and G. K. Lahiri, *Dalton Trans.*, 2015, **44**, 13204; (g) A. Das, H. Agarwala, T. Kundu, P. Ghosh, S. Mondal, S. M. Mobin and G. K. Lahiri, *Dalton Trans.*, 2014, **43**, 13932; (i) C. Bhaumik, D. Maity, S. Das and S. Baitalik, *Polyhedron*, 2013, **52**, 890; (j) D. Saha, S. das, D. Maity and S. Baitalik, *Indian J. Chem., Sect. A*, 2011, **50A**, 1418.

- 8 Selected recent references: (a) W.-X. Ni, W.-L. Man, S.-M. Yiu, M. Ho, M. T.-W. Cheung, C.-C. Ko, C.-M. Che, Y.-W. Lam and T.-C. Lau, *Chem. Sci.*, 2012, **3**, 1582; (b) M. Schmidlehner, P.-S. Kuhn, C. M. Hackl, A. Roller, W. Kandioller and B. K. Keppler, *J. Organomet. Chem.*, 2014, **772**, 93; (c) G. E. Büchel, A. Gavriluta, M. Novak, S. M. Meier, M. A. Jakupec, O. Cuzan, C. Turta, J.-B. Tommasino, E. Jeanneau, G. Novitchi, D. Luneau and V. B. Arion, *Inorg. Chem.*, 2013, **52**, 6273; (d) G. E. Büchel, I. N. Stepanenko, M. Hejl, M. A. Jakupec, V. B. Arion and B. K. Keppler, *Inorg. Chem.*, 2009, **48**, 10737; (e) P.-S. Kuhn, G. E. Büchel, K. K. Jovanović, L. Filipović, S. Radulović, P. Raptá and V. B. Arion, *Inorg. Chem.*, 2014, **53**, 11130; (f) R. Schuecker, R. O. John, M. A. Jakupec, V. B. Arion and B. K. Keppler, *Organometallics*, 2008, **27**, 6587; (g) A. Egger, B. Cebrián-Losantos, I. N. Stepanenko, A. A. Krokhin, R. Eichinger, M. A. Jakupec, V. B. Arion, B. K. Keppler, *Chem. Biodivers*, 2008, **5**, 1588. (h) B. K. Bennett, S. J. Pitteri, L. Pilobello, S. Lovell, W. Kaminsky, J. M. Mayer, *Dalton Trans.*, 2001, 3489; (i) G. Albertin, S. Antoniutti, J. Castro and S. García-Fontán, *Eur. J. Inorg. Chem.*, 2011, 510; (j) K. Chen, Y.-M. Cheng, Y. Chi, M.-L. Ho, C.-H. Lai, P.-T. Chou, S.-M. Peng, G.-H. Lee, *Chem. Asian J.*, 2007, **2**, 155; (k) T. J. Crevier, S. Lovell, J. M. Mayer, *Chem. Commun.*, 1998, 2371; (l) S. Baitalik, S. Dutta, P. Biswas, U. Flürke, E. Bothe, K. Nag, *Eur. J. Inorg.*

- Chem.*, 2010, 570; (m) Y. Chi, H.-L. Yu, W.-L. Ching, C.-S. Liu, Y.-L. Chen, T.-Y. Chou, S.-M. Peng, G.-H. Lee, *J. Mater. Chem.*, 2002, **12**, 1363.
- 9 (a) L. Zang and S. Jiang, *SpectrochimActa, Part A: Mol. Biomol. Spectrosc.*, 2015, **150**, 814; (b) P. Ghosh, B. G. Roy, S. Jana, S. K. Mukhopadhyay and P. Banerjee, *Phys. Chem. Chem. Phys.*, 2015, **17**, 20288; (c) D. Curiel, A. Cowley and P. D. Beer, *Chem. Commun.*, 2005, 236; (d) M. Cigáň, K. Jakusová, J. Donovalová, V. Szöcs and A. Gápslovský, *RSC Adv.*, 2014, **4**, 54072; (e) T. Mizuno, W.-H. Wei, L. R. Eller and J. L. Sessler, *J. Am. Chem. Soc.*, 2002, **124**, 1134; (f) I. V. Korendovych, R. A. Roesner and E. V. Rybak-Akimova, *Adv. Inorg. Chem.*, 2007, **59**, 109; (g) F. Otón, A. Espinosa, A. Tárraga, I. Ratera, K. Wurst, J. Veciana and P. Molina, *Inorg. Chem.*, 2009, **48**, 1566; (h) P. Dydio, T. Zielinski and J. Jurczak, *J. Org. Chem.*, 2009, **74**, 1525; (i) M. Boiocchi, L. D. Boca, D. Esteban-Gómez, L. Fabbrizzi, M. Licchelli and E. Monzani, *J. Am. Chem. Soc.*, 2004, **126**, 16507; (j) L. S. Evans, P. A. Gale, M. E. Light and R. Quesada, *Chem. Commun.*, 2006, 965; (k) V. S. Bryantsev and B. P. Hay, *J. Am. Chem. Soc.*, 2006, **128**, 2035; (l) B. P. Hay, T. K. Firman and B. A. Moyer, *J. Am. Chem. Soc.*, 2005, **127**, 1810.
- 10 (a) P. Mondal, S. Plebst, R. Ray, S. M. Mobin, W. Kaim and G. K. Lahiri, *Inorg. Chem.*, 2014, **53**, 9348; (b) P. Mondal, H. Agarwala, R. D. Jana, S. Plebst, A. Grupp, F. Ehret, S. M. Mobin, W. Kaim and G. K. Lahiri, *Inorg. Chem.*, 2014, **53**, 7389.
- 11 (a) S. Ye, B. Sarkar, C. Duboc, J. Fiedler and W. Kaim, *Inorg. Chem.*, 2005, **44**, 2843; (b) E. C. Constable, P. R. Raithby, D. N. Smit, *Polyhedron*, 1989, **8**, 367.
- 12 (a) I. N. Stepanenko, B. Cebrián-Losantos, V. B. Arion, A. A. Krokhin, A. A. Nazarov and B. K. Keppler, *Eur. J. Inorg. Chem.*, 2007, 400; (b) M. A. Esteruelas, F. J. Lahoz, L. A. Oro, E. Oñate and N. Ruiz, *Inorg. Chem.*, 1994, **33**, 787; (c) S. Baitalik, U. Florke, K.



- Nag, *Inorg. Chim. Acta*, 2002, **337**, 439; (e) S. Baitalik, P. Bag, U. Florke, K. Nag, *Inorg. Chim. Acta*, 2004, **357**, 699; (f) S.-H. Chang, C.-F. Chang, J.-L. Liao, Y. Chi, D.-Y. Zhou, L.-S. Liao, T.-Y. Jiang, T.-P. Chou, E. Y. Li, G.-H. Lee, T.-Y. Kuo and P.-T. Chou, *Inorg. Chem.*, 2013, **52**, 5867.
- 13 (a) M. A. Esteruelas, C.-G. Yebra, M. Olivan, E. Oñate and M. Valencia, *Organometallics*, 2008, **27**, 4892; (b) C. Ye and T. B. Wen, *Acta Crystallogr. Sect. E*, 2009, **E65**, m1242; (c) F. A. Cotton, A. R. Chakravarty and D. A. Tocher, *Inorg. Chim. Acta*, 1984, **87**, 115.
- 14 (a) P. Ghosh, R. Ray, A. Das and G. K. Lahiri, *Inorg. Chem.*, 2014, **53**, 10695; (b) D. Das, T. M. Scherer, A. Das, T. K. Mondal, S. M. Mobin, J. Fiedler, J. L. Priego, R. Jiménez-Aparicio, W. Kaim and G. K. Lahiri, *Dalton Trans.*, 2012, **41**, 11675; (c) G. K. Lahiri, S. Bhattacharya, B. K. Ghosh and A. Chakravorty, *Inorg. Chem.*, 1987, **26**, 4324.
- 15 (a) B. C. Losantos, A. A. Krokhin, I. N. Stepanenko, R. Eichinger, M. A. Jakupec, V. B. Arion and B. K. Keppler, *Inorg. Chem.*, 2007, **46**, 5023; (b) I. N. Stepanenko, A. A. Krokhin, R. O. John, A. Roller, V. B. Arion, M. A. Jakupec and B. K. Keppler, *Inorg. Chem.*, 2008, **47**, 7338; (c) B. Wu, X. Huang, Y. Xia, Y.; X.-J. Yang and C. Janiak, *CrystEngComm.*, 2007, **9**, 676; (f) M. Seredyuk, M. Haukka, V. A. Pavlenko and I. O. Fritsky, *Acta Crystallogr. Sect. E*, 2009, **65**, m1396; (g) D. B. Grotjahn, S. Van, D. Combs, W. S. Kassel and A. L. Rheingold, *J. Inorg. Biochem.*, 2001, **85**, 61; (h) Y. Baran, H. Esener and M. Turkyilmaz, *Synth. React. Inorg. M.*, 2011, **41**, 710.
- 16 (a) F. H. Beijer, H. Kooijman, A. L. Spek, R. P. Sijbesma and E. W. Meijer, *Angew. Chem., Int. Ed.*, 1998, **37**, 75; (b) E. Arunan, G. R. Desiraju, R. A. Klein, J. Sadlej, S. Schneiner, I. Alkorta, D. C. Clary, R. H. Crabtree, J. J. Dannenberg, P. Hobza, H. G. Kjaergaard, A. C. Legon, B. Mennucci and D. J. Nebitt, *Pure Appl. Chem.*, 2011, **83**, 1637;

- (c) W.-K. Li, G.-D. Zhou, T. C. W. M. Mak, *Advanced Structural Inorganic Chemistry*; Oxford Publishing: New York, 2008, p. 403.
- 17 H. Jude, F. N. Rein, W. Chen, B. L. Scott, D. M. Dattelbaum and R. C. Rocha, *Eur. J. Inorg. Chem.*, 2009, 683.
- 18 (a) A. Das, T. M. Scherer, S. M. Mobin, W. Kaim and G. K. Lahiri, *Inorg. Chem.*, 2012, **51**, 4390; (b) A. Das, T. M. Scherer, P. Mondal, S. M. Mobin, W. Kaim and G. K. Lahiri, *Chem. -Eur. J.*, 2012, **18**, 14434; (c) A. Mandal, T. Kundu, F. Ehret, M. Bubrin, S. M. Mobin, W. Kaim and G. K. Lahiri, *Dalton Trans.*, 2014, **43**, 2473; (d) P. Mondal, R. Ray, A. Das and G. K. Lahiri, *Inorg. Chem.*, 2015, **54**, 3012; (e) A. Das, P. Ghosh, S. Plebst, B. Schwederski, S. M. Mobin, W. Kaim and G. K. Lahiri, *Inorg. Chem.*, 2015, **54**, 3376.
- 19 (a) J. A. Weil, J. R. Bolton and J. E. Wertz, *Electron Paramagnetic Resonance*, Wiley Publishing: New York, 1994, p. 532; (b) W. Kaim, B. Sarkar, *Coord. Chem. Rev.*, 2013, **257**, 1650.
- 20 (a) P. Ghosh, P. Mondal, R. Ray, A. Das, S. Bag, S. M. Mobin and G. K. Lahiri, *Inorg. Chem.*, 2014, **53**, 6094; (b) A. Pramanik, N. Bag, D. Ray, G. K. Lahiri and A. Chakravorty, *Inorg. Chem.*, 1991, **30**, 410.
- 21 J. J. Concepcion, M. D. Dattelbaum, T. J. Meyer and R. C. Rocha, *Philos. Trans. R. Soc. London*, 2008, **366**, 163.
- 22 (a) Z. Yang, K. Zhang, F. Gong, S. Li, J. Chen, J. S. Ma, L. N. Sobenina, A. I. Mikhaleva, G. Yang and B. A. Trofimov, *Beilstein J. Org. Chem.*, 2011, **7**, 46; (b) T.-P. Lin, C.-Y. Chen, Y.-S. Wen and S.-S. Sun, *Inorg. Chem.*, 2007, **46**, 9201.
- 23 (a) N. Kumari, S. Jha and S. Bhattacharya, *J. Org. Chem.*, 2011, **76**, 8215; (b) L. Wang, W. Wei, Y. Guo, J. Xu and S. Shao, *Spectrochim Acta, Part A: Mol. Biomol. Spectrosc.*, 2011,

- 78, 726.
- 24 (a) R. Pegu, R. Mandal, A. K. Guha and S. Pratihari, *New J. Chem.*, 2015, **39**, 5984; (b) S. O. Kang, D. Powell, V. W. Day and K. Bowman-James, *Angew. Chem., Int. Ed.*, 2006, **45**, 1921; (c) B. Kumar, M. A. Kaloo, A. R. Sekhar and J. Sankar, *Dalton Trans.*, 2014, **43**, 16164; (d) P. Bose and P. Ghosh, *Chem. Commun.*, 2010, **46**, 2962; (e) H. D. P. Ali, S. J. Quinn, T. McCabe, P. E. Kruger and T. Gunnlaugsson, *New J. Chem.*, 2009, **33**, 793.
- 25 (a) C.-I. Lin, S. Selvi, J.-M. Fang, P.-T. Chou, C.-H. Lai and Y.-M. Cheng, *J. Org. Chem.*, 2007, **72**, 3537; (b) Z. Xu, N. J. Singh, S. K. Kim, D. R. Spring, K. S. Kim and J. Yoon, *Chem. -Eur. J.*, 2011, **17**, 1163.
- 26 (a) M. D. C. González, F. Otón, A. Espinosa, A. Tárraga and P. Molina, *Org. Biomol. Chem.*, 2015, **13**, 1429; (b) J. A. Drewry, S. Fletcher, H. Hassan and P. Gunning, *Org. Biomol. Chem.*, 2009, **7**, 5074; (c) P. Bose, R. Dutta, S. Santra, B. Chowdhury and P. Ghosh, *Eur. J. Inorg. Chem.*, 2012, 5791; (d) J. Yoo, M.-S. Kim, S.-J. Hong, J. L. Sessler and C.-H. Lee, *J. Org. Chem.*, 2009, **74**, 1065; (e) P.A. Gale, N. Busschaert, C. J. E. Haynes, L. E. Karagiannidis and I. L. Kirby, *Chem. Soc. Rev.*, 2014, **43**, 205.
- 27 T. Banerjee, S. K. Singh and N. Kishore, *J. Phys. Chem. B*, 2006, **110**, 24147.
- 28 P. D. Ross and S. Subramanian, *Biochemistry*, 1981, **20**, 3096.
- 29 (a) M. Boiocchi, L. Del Boca, D. Esteban-Gómez, L. Fabbrizzi, M. Licchelli and E. Monzani, *Chem.-Eur. J.*, 2005, **11**, 3097; (b) D. Esteban-Gómez, L. Fabbrizzi, M. Licchelli and E. Monzani, *Org. Biomol. Chem.*, 2005, **3**, 1495.
- 30 (a) T. Kundu, S. M. Mobin and G. K. Lahiri, *Dalton Trans.*, 2010, **39**, 4232; (b) Y. Cui, H.-J. Mo, J.-C. Chen, Y.-L. Niu, Y.-R. Zhong, K.-C. Zheng and B.-H. Ye, *Inorg. Chem.*, 2007, **46**, 6427; (c) D. F. Shriver and P. W. Atkins, *Inorganic Chemistry*, Oxford

- University Press, 3rd edn, 1999; (d) T. D. B. Morgan, G. Stedman and P. A. E. Whincup, *J. Chem. Soc.*, 1965, 4813; (e) T. I. Crowell and M. G. Hankins, *J. Phys. Chem.*, 1969, **73**, 1380.
- 31 P. A. Lay, M. Sargeson and H. Taube, *Inorg. Synth.*, 1986, **24**, 291.
- 32 (a) Y. Liu, B. -H. Han and Y. -T. Chen, *J. Phys. Chem. B*, 2002, **106**, 4678; (b) Y. Liu, B. -H. Han, S. -X. Sun, T. Wada and Y. Inoue, *J. Org. Chem.*, 1999, **64**, 1487; (c) C. Basu, S. Biswas, A. P. Chattopadhyay, H. Stoeckli-Evans and S. Mukherjee, *Eur. J. Inorg. Chem.*, 2008, 4927; (d) L. Wang, X.-J. Zhu, W.-Y. Wong, J.-P. Guo, W.-K. Wong and Z.-Y. Li, *Dalton Trans.*, 2005, 3235; (e) B. Valeur, J. Pouget, J. Bouson, M. Kaschke and N. P. Ernsting, *J. Phys. Chem.*, 1992, **96**, 6545; (f) Y. Liu, B. Li, C.-C. You, T. Wada and Y. Inoue, *J. Org. Chem.*, 2001, **66**, 225.
- 33 (a) G. M. Sheldrick, *Acta Crystallogr. Sect. A*, 2008, **A64**, 112; (b) *Program for Crystal Structure Solution and Refinement*, University of Goettingen: Goettingen, Germany, 1997; (c) G. M. Sheldrick, *Acta Crystallogr. Sect. C*, 2015, **C71**, 3.
- 34 C. Lee, W. Yang and R. G. Parr, *Phys. Rev. B*, 1988, **37**, 785.
- 35 (a) D. Andrae, U. Haeussermann, M. Dolg, H. Stoll and H. Preuss, *Theor. Chim. Acta*, 1990, **77**, 123; (b) P. Fuentealba, H. Preuss, H. Stoll and L. V. Szentpaly, *Chem. Phys. Lett.*, 1989, **89**, 418.
- 36 M. J. Frisch, G. W. Trucks, H. B. Schlegel, G. E. Scuseria, M. A. Robb, J. R. Cheeseman, G. Scalmani, V. Barone, B. Mennucci, G. A. Petersson, H. Nakatsuji, M. Caricato, X. Li, H. P. Hratchian, A. F. Izmaylov, J. Bloino, G. Zheng, J. L. Sonnenberg, M. Hada, M. Ehara, K. Toyota, R. Fukuda, J. Hasegawa, M. Ishida, T. Nakajima, Y. Honda, O. Kitao, H. Nakai, T. Vreven, J. A. Montgomery, Jr. J. E. Peralta, F. Ogliaro, M. Bearpark, J. J.

- Heyd, E. Brothers, K. N. Kudin, V. N. Staroverov, R. Kobayashi, J. Normand, K. Raghavachari, A. Rendell, J. C. Burant, S. S. Iyengar, J. Tomasi, M. Cossi, N. Rega, J. M. Millam, M. Klene, J. E. Knox, J. B. Cross, V. Bakken, C. Adamo, J. Jaramillo, R. Gomperts, R. E. Stratmann, O. Yazyev, A. J. Austin, R. Cammi, C. Pomelli, J. W. Ochterski, R. L. Martin, K. Morokuma, V. G. Zakrzewski, G. A. Voth, P. Salvador, J. J. Dannenberg, S. Dapprich, A. D. Daniels, O. Farkas, J. B. Foresman, J. V. Ortiz, J. Cioslowski and D. J. Fox, *Gaussian 09 (Revision A.02)*: Gaussian, Inc.: Wallingford CT 2009.
- 37 (a) R. Bauernschmitt and R. Ahlrichs, *Chem. Phys. Lett.*, 1996, **256**, 454; (b) R. E. Stratmann, G. E. Scuseria and M. J. Frisch, *J. Chem. Phys.*, 1998, **109**, 8218; (c) M. E. Casida, C. Jamorski, K. C. Casida and D. R. Salahub, *J. Chem. Phys.*, 1998, **108**, 4439.
- 38 (a) V. Barone and M. Cossi, *J. Phys. Chem. A*, 1998, **102**, 1995; (b) M. Cossi and V. Barone, *J. Chem. Phys.*, 2001, **115**, 4708; (c) M. Cossi, N. Rega, G. Scalmani and V. Barone, *J. Comput. Chem.*, 2003, **24**, 669.
- 39 S. Leonid, *Chemissian 1.7*. 2005-2010. Available at <http://www.chemissian.com>.
- 40 D. A. Zhurko, G. A. Zhurko, *ChemCraft 1.5*; Plimus: San Diego, CA. Available at <http://www.chemcraftprog.com>.

## Table of Contents

### **Substituent directed selectivity in anion recognition by a new class of simple osmium-pyrazole derived receptor**

Ankita Das, Prasenjit Mondal, Moumita Dasgupta, Nand Kishore\* and Goutam Kumar Lahiri\*

*Department of Chemistry, Indian Institute of Technology Bombay, Powai, Mumbai-400076, India. E-mail: [lahiri@chem.iitb.ac.in](mailto:lahiri@chem.iitb.ac.in)*

Remarkable impact of 3,5-dimethylpyrazole derived osmium framework with hydrogen bonded NH for the selective recognition of F<sup>-</sup> has been ascertained.

